
Clin-JEPA: A Multi-Phase Co-Training Framework for Joint-Embedding Predictive Pretraining on EHR Patient Trajectories

Yixuan Yang* Mehak Arora Ryan Zhang Baraa Abed Junseob Kim
 Tilendra Choudhary Md Hassanuzzaman Kevin Zhu Ayman Ali Chengkun Yang
 Alasdair Edward Gent Victor Moas Rishikesan Kamaleswaran
 Duke University, Durham, NC, USA

Abstract

We present CLIN-JEPA, a multi-phase co-training framework for joint-embedding predictive (JEPA) pretraining on electronic health record (EHR) patient trajectories. JEPA architectures have enabled latent-space planning in robotics and high-quality representation learning in vision, but extending the paradigm to EHR data—to obtain a single backbone that simultaneously forecasts patient trajectories and serves diverse downstream risk-prediction tasks without per-task fine-tuning—remains an open challenge. Existing JEPA frameworks either discard the predictor after pretraining (I-JEPA, V-JEPA) or train it on a frozen pretrained encoder (V-JEPA 2-AC), leaving the encoder unaware of the rollout signal that the retained predictor must use at inference; co-training the encoder and predictor under a shared JEPA prediction objective would supply this grounding, but naïve co-training is unstable, with representation collapse and online/target drift causing autoregressive rollout to diverge. CLIN-JEPA’s five-phase pretraining curriculum—predictor warmup, joint refinement, EMA target alignment, hard sync, and predictor finalization—addresses each failure mode by phase, stably co-training a Qwen3-8B-based encoder and a 92M-parameter latent trajectory predictor. On MIMIC-IV ICU data, three independent evaluations support the framework: (1) latent ℓ_1 rollout drift uniquely *converges* (-15.7%) over 48-hour horizons while baselines and ablations diverge ($+3\%$ to $+4951\%$); (2) the encoder learns a clinically discriminative latent geometry (deteriorating-patient cohorts displace $4.83\times$ further than stable patients in latent space, vs $\leq 2.62\times$ for baseline encoders); (3) a single backbone outperforms strong tabular and sequence baselines on multi-task downstream evaluation. CLIN-JEPA achieves mean AUROC 0.851 on ICareFM EEP and 0.883 on 8 binary risk tasks ($+0.038$ and $+0.041$ vs baseline average).

1 Introduction

A patient’s stay in the intensive care unit (ICU) is a high-dimensional dynamical system: every hour brings new vital signs, laboratory values, and clinical interventions whose effects on patient state must be accounted for in both forecasting and risk prediction. Existing electronic-health-record (EHR) modelling approaches address only part of this problem. Token-autoregressive language models trained on tokenised EHR sequences [1–4] can generate plausible event trajectories, but treat the patient as a sequence of static text events and never explicitly model the underlying continuous physiological state. Per-task foundation models for the ICU [5] achieve strong task-level performance,

*Corresponding author: yixuan.yang@duke.edu

Code: <https://github.com/YeungYathin/Clin-JEPA>

but require per-task feature engineering and fine-tuning with no unified representation that supports trajectory simulation.

Recent latent world models in vision and robotics offer a promising direction. Joint-Embedding Predictive Architectures (JEPA) [6–8] pre-train representations by predicting masked or future content in a latent space rather than reconstructing pixels, and V-JEPA 2-AC [9] retains an action-conditioned predictor at inference to enable latent-space rollout for robotic planning. Adapting this paradigm to clinical EHR—where the analogous goal is a patient-state simulator that consumes free-text observations and interventions—is appealing but non-trivial.

Existing JEPA designs leave the inference-time-simulator use case open. I-JEPA [7] and V-JEPA [8] discard the predictor after pretraining, so only the encoder is available downstream and trajectory simulation is impossible. V-JEPA 2-AC [9] retains the predictor but trains it on a *frozen* pretrained encoder, leaving the encoder unaware of the rollout signal that the retained predictor must use at inference. Co-training the encoder and predictor under a shared JEPA prediction objective would simultaneously close both gaps—producing an encoder whose representations are dynamically grounded for the predictor, and a predictor that operates in a representation space jointly optimized for it. However, naïve co-training is unstable: the encoder is dragged toward representation collapse by an untrained predictor, and the predictor’s autoregressive rollout diverges as it accumulates errors in a moving target latent space.

We present CLIN-JEPA, a multi-phase co-training framework that closes this gap. Our contributions are: (1) a five-phase pretraining curriculum (predictor warmup, joint encoder–predictor refinement, EMA target alignment, hard sync, and predictor finalization) that stably co-trains a Qwen3-8B-based encoder with a retained latent trajectory predictor on MIMIC-IV ICU data [10]; (2) a text-based EHR representation that consumes raw clinical text and serves all downstream tasks from a single set of latent embeddings, requiring no missing-value imputation, no normalization, and no hand-engineered features; and (3) a three-axis empirical evaluation showing that CLIN-JEPA uniquely converges over a 48-hour autoregressive horizon, learns a clinically discriminative latent geometry that separates deteriorating from stable patient cohorts, and outperforms strong tabular and sequence baselines on two standard ICU benchmarks. The framework is summarized in Figure 1.

2 Related Work

Clinical foundation models for EHR. Pretrained models for EHR span early encoder-only architectures such as Med-BERT [11] (structured ICD code sequences) and GatorTron [12] (clinical-text encoder), generative or autoregressive trajectory models [1, 2, 13, 14], and reasoning-enhanced or instruction-tuned LLMs for EHR analysis [3, 4, 15]. Multi-task ICU foundation models [5, 16, 17] achieve strong task-level performance through zero-shot in-context evaluation or per-task fine-tuning; recent empirical analysis [18] documents cross-institution transferability challenges. Across these architectures, none provides an explicit latent dynamical state representation suitable for autoregressive trajectory simulation.

JEPA paradigm. Joint-embedding predictive architectures (JEPA) [6] were realized for vision in I-JEPA [7] and V-JEPA [8], then extended with a retained action-conditioned predictor for robotic planning (V-JEPA 2-AC [9]), to language (LLM-JEPA [19]), and to vision-language (VL-JEPA [20]). The closest medical adaptation, SMB-Structure [21], jointly applies SFT and JEPA over masked future-token spans on longitudinal oncology EHR with an LLM encoder, but uses only the encoder’s embeddings for downstream tasks via linear probes.

Latent world models for clinical decision support. A parallel line of work introduces explicit latent world models for ICU and oncology decision support. medDreamer [22] adopts a Dreamer-style [23] RSSM trained from scratch with a discrete action space for sepsis policy learning. Latent Physiology as Language [24] models patients as a continuous-time latent SDE with EHR events as control inputs, trained jointly with reconstruction, masked imputation, and intervention-aware rollout-consistency objectives. CLARITY [25] pairs a LoRA-adapted MRI foundation encoder with an action-conditioned latent predictor on brain-tumor and breast-cancer MRI cohorts. The Qazi et al. [26] survey reviews this emerging paradigm. None of the above jointly grounds an LLM encoder against the rollout signal of a retained latent predictor — the gap CLIN-JEPA closes with a multi-phase co-training curriculum.

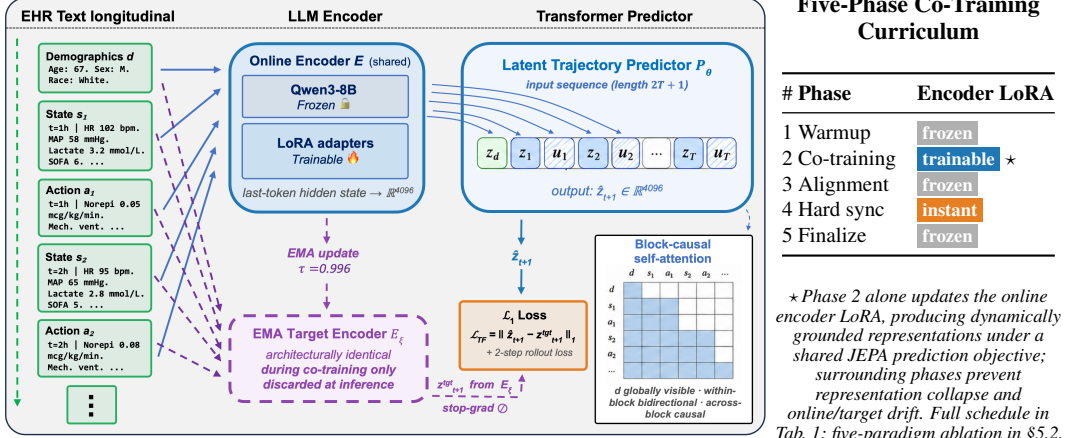


Figure 1: **The CLIN-JEPA framework.** (Left) Three text inputs (demographics d , per-hour state s_t , action a_t) are processed by a single shared encoder E — Qwen3-8B base (frozen) with LoRA adapters (trainable) — producing 4096-dim latent embeddings via last-token extraction. The latent trajectory predictor P_θ is a block-causal Transformer that consumes the interleaved sequence $[z_d, z_1, u_1, z_2, u_2, \dots, z_T, u_T]$ and outputs \hat{z}_{t+1} . The EMA target encoder E_ξ (dashed purple, training-only) provides a stop-gradient anchor for the ℓ_1 teacher-forcing loss; at inference, E_ξ is discarded and $E + P_\theta$ run autoregressively, chaining \hat{z}_{t+h} back as next-step state input. (Right) Five-phase pretraining curriculum: only Phase 2 (\star) updates the online encoder LoRA, with surrounding phases preventing the two failure modes that derail naïve co-training.

3 Clin-JEPA Framework

The CLIN-JEPA framework comprises two deployed components illustrated in Figure 1: an LLM-based encoder that maps EHR text into a continuous latent space, and a Transformer that autoregressively predicts patient trajectories in that latent space. §3.1 introduces the problem formulation and encoder; §3.2 details the latent trajectory predictor.

3.1 Problem Formulation and Patient State Encoding

A patient’s ICU stay constitutes a longitudinal EHR sequence of clinical events—observations (vital signs, laboratory measurements, severity scores) and interventions (medications, ventilator settings, procedures). We model each stay over a 72-hour window discretized into one-hour bins (consistent with the 24–72 h analysis windows commonly used in ICU forecasting literature [27, 28]). This yields a sequence of state–action pairs of length $T \leq 72$ preceded by a static demographics descriptor d available at admission:

$$\mathcal{S} = \{d, (s_1, a_1), (s_2, a_2), \dots, (s_T, a_T)\}, \quad (1)$$

where s_t records all observations occurring during hour t in their original temporal order and a_t enumerates the clinical interventions active during hour t .

We represent state s_t , action a_t , and demographics d as structured natural-language text fragments rather than fixed numerical vectors. This unifies heterogeneous EHR signals (vitals, labs, drugs, procedures) under a single text representation, leverages the LLM’s pretrained linguistic knowledge, and preserves human readability for clinical interpretation. The state text concatenates one hour’s clinical readings (such as vital signs, laboratory values, severity scores), e.g., “t=12h | Heart rate: 88 bpm. MAP: 62 mmHg. Lactate: 2.1 mmol/L. ...”. The action text enumerates active interventions and doses, e.g., “t=12h | Norepinephrine: 0.08 mcg/kg/min. Propofol: 40 mcg/kg/min. ...”. Within each hour we preserve every individual reading in its original temporal order—including repeated measurements of the same variable (e.g., MAP sampled multiple times during resuscitation)—as a lossless serialization that the encoder’s self-attention parses for intra-hour dynamics; the latent trajectory predictor (§3.2) then composes these per-hour embeddings into inter-hour dynamics. This representation requires no value imputation, no normalization, and no modality-specific featurization: missing readings are simply absent from the state text, and numeric values appear in their natural clinical units.

Each of the three text inputs (state s_t , action a_t , and demographics d) is independently mapped to a 4096-dimensional latent embedding by our encoder E : a Qwen3-8B language model whose base weights are frozen and adapted via lightweight LoRA adapters. The same shared encoder processes state, action, and demographics text via independent forward passes, with the last-token hidden state taken as the embedding:

$$z_t = E(s_t), \quad u_t = E(a_t), \quad z_d = E(d), \quad z_t, u_t, z_d \in \mathbb{R}^{4096}. \quad (2)$$

The LoRA adapters are first initialized via supervised next-token-prediction fine-tuning on per-hour state and action text, then refined jointly with the latent trajectory predictor (§3.2) under the multi-phase co-training curriculum (§4). LoRA configuration and training compute are reported in §5.1.

CLIN-JEPA’s central objective is to predict the patient’s future latent trajectory over an H -hour horizon given past context and a proposed action sequence, autoregressively in the encoder’s \mathbb{R}^{4096} latent space:

$$\hat{z}_{t+h} = P_\theta(\tilde{z}_{1:t+h-1}, u_{1:t+h-1}, z_d), \quad h = 1, \dots, H, \quad (3)$$

where $\tilde{z}_j = z_j$ for $j \leq t$ (encoded ground truth) and $\tilde{z}_j = \hat{z}_j$ for $j > t$ (the predictor’s own prior output, fed back at each rollout step), and P_θ is the latent trajectory predictor (§3.2). The encoded history $\{z_1, \dots, z_t\}$ together with the autoregressive rollout $\{\hat{z}_{t+h}\}_{h=1}^H$ jointly serves as the patient-state representation for downstream clinical tasks.

3.2 Latent Trajectory Predictor

The latent trajectory predictor P_θ is a Transformer encoder (~ 92 M parameters) that operates entirely in the 4096-dim encoder latent space. It consumes the demographics-state-action sequence $[z_d, z_1, u_1, z_2, u_2, \dots, z_T, u_T]$ of length $2T + 1$, where z_d occupies position 0 as a global context token and (z_t, u_t) pairs occupy positions $(2t - 1, 2t)$. Before entering the Transformer, each encoder embedding is projected from \mathbb{R}^{4096} to the predictor’s hidden dimension \mathbb{R}^{1024} by one of three modality-specific linear maps—one for state, one for action, one for demographics:

$$h_t^{(s)} = W_s z_t, \quad h_t^{(a)} = W_a u_t, \quad h_d = W_d z_d, \quad W_s, W_a, W_d \in \mathbb{R}^{1024 \times 4096}, \quad (4)$$

and a learned absolute positional embedding is added to $h_t^{(s)}, h_t^{(a)}, h_d$ at each position.

Self-attention is block-causal (Figure 1, mask inset): demographics is globally visible; tokens within a timestep block attend bidirectionally; across blocks attention is strictly causal. An output linear projection yields the absolute next-state prediction $\hat{z}_{t+1} \in \mathbb{R}^{4096}$ from each state position.

At inference, P_θ is retained and rolls out autoregressively: each predicted \hat{z}_{t+h} is fed back as the state input for step $t + h + 1$, yielding the simulated trajectory $\{\hat{z}_{t+h}\}_{h=1}^H$ used for downstream clinical tasks (Eq. 3). Unlike token-LM autoregression, which samples a discrete token and feeds the sample back, our rollout feeds back the predicted continuous embedding directly—a deterministic conditional-mean composition that lets a single predictor cover all forecast horizons $h=1, \dots, H$ with one shared model rather than training H horizon-specific predictors.

4 Multi-Phase Co-Training Pretraining

Building on the SFT-initialized encoder of §3.1, we jointly co-train the encoder LoRA adapters and the latent trajectory predictor under a shared JEPA prediction objective. This co-training is motivated by CLIN-JEPA’s deployment regime: unlike I-JEPA [7] and V-JEPA [8], which discard the predictor after pretraining, our predictor is retained at inference and rolls out autoregressively to simulate patient trajectories. For these rollouts to produce clinically faithful dynamics, the encoder cannot only learn statically rich features (the regime image and video JEPA optimize for); it must learn representations that are *dynamically grounded* — organized so that the predictor can compose them into long autoregressive trajectories. Sharing a single JEPA prediction objective between encoder and predictor is what produces this grounding, and it is what distinguishes our framework from V-JEPA 2-AC [9], where the predictor is trained on a frozen pretrained encoder and the encoder never sees the rollout signal.

This co-training is, however, unstable in the shared latent space: a naïve implementation leads to two characteristic failure modes — *representation collapse* (the encoder degenerates to constant outputs

Table 1: The five-phase co-training curriculum; per-component ablation in §5.2. \equiv denotes parameter equality between online and target encoders.

Phase	Encoder LoRA	Target encoder	Rollout regime	Purpose of this phase
1. Warmup	frozen	online \equiv target (init)	Native	Predictor warmstart on SFT-initialized encoder
2. Co-training	trainable	EMA target, slow	Teacher-forced	Encoder + predictor jointly refined under stable target
3. Alignment	frozen	EMA chases online	Teacher-forced	Target encoder smoothly catches up to online
4. Hard sync	— (instant)	target \leftarrow online	—	Eliminate residual online–target mismatch
5. Finalize	frozen	online \equiv target (post-sync)	Native	Extended predictor training to convergence on stable encoder

the predictor can match trivially) and *online/target space drift* (the predictor learns to forecast in a moving target latent space and diverges under autoregressive rollout). §4.1 formalizes the co-training objective and the EMA target encoder used to keep prediction targets stable; §4.2 introduces the five-phase schedule that prevents each failure mode by phase.

4.1 Co-Training Objective

The predictor is trained to minimize the ℓ_1 distance between its predicted next-state embedding and the target encoder’s embedding of the actual next state. Letting \mathcal{V} denote the set of valid (sample b , time t) pairs in a training batch, the teacher-forcing loss is

$$\mathcal{L}_{\text{TF}} = \frac{1}{|\mathcal{V}|} \sum_{(b,t) \in \mathcal{V}} \|\hat{z}_{t+1}^{(b)} - z_{t+1}^{\text{target},(b)}\|_1, \quad (5)$$

where $\|\cdot\|_1$ denotes the ℓ_1 norm summed over the embedding’s 4096 dimensions. The total per-step training loss combines this with a short autoregressive rollout loss, $\mathcal{L} = \mathcal{L}_{\text{TF}} + \mathcal{L}_{\text{roll}}$, where $\mathcal{L}_{\text{roll}}$ averages the same ℓ_1 penalty over a 2-step autoregressive horizon (using the rollout in Eq. 3) to encourage stability under multi-step inference. Following prior JEPA work [7, 8], we use ℓ_1 rather than MSE for robustness to heavy-tailed clinical laboratory distributions.

Following the JEPA family [7–9], we maintain a separate *target encoder* that is architecturally identical to the online encoder (frozen Qwen3-8B with LoRA adapters) and updated as an exponential moving average of the online encoder’s parameters: $\theta_{\text{target}} \leftarrow \tau \theta_{\text{target}} + (1 - \tau) \theta_{\text{online}}$, applied at each optimizer step with momentum $\tau = 0.996$ (matching I-JEPA’s default). The target encoder serves only as a stop-gradient anchor for z_{t+1}^{target} , carries no projection head, and is discarded entirely at inference.

The rollout loss admits two regimes depending on whether the online and target encoders agree. *Native rollout* (used when online \equiv target) chains the predictor’s own output back as the next-step state input, mirroring inference behaviour. *Teacher-forced rollout* (used in phases where online \neq target) instead substitutes the real online embedding at each rollout step; this prevents a space-mismatch failure where chained predictor outputs (trained to land in target space) would be fed back into a pipeline that expects online-space inputs.

4.2 Five-Phase Curriculum

Table 1 summarizes the five-phase schedule, which we describe in turn.

Phase 1 (Warmup). The predictor is trained alone against the frozen SFT-initialized encoder, warming up the cold predictor on initial trajectory dynamics before any encoder co-adaptation. Without this warmup, the cold predictor would, when the encoder unlocks in Phase 2, immediately exert a strong gradient pull dragging the encoder toward trivial constant embeddings — the representation-collapse failure mode. **Phase 2 (Co-training).** This is the central refinement step of the curriculum: the encoder LoRA adapters are unlocked and optimized together with the predictor under the same JEPA prediction objective, with teacher-forced rollout sidestepping the space mismatch described in §4.1. It is the only phase in which the predictor’s gradient signal reaches the encoder, and therefore the phase

where the encoder’s representations actually become *dynamically grounded*. **Phase 3 (Alignment)**. The online encoder is re-frozen and the EMA target smoothly catches up to it. This soft alignment serves as a buffer before the explicit hard sync in Phase 4, preventing an abrupt parameter jump that would destabilize the predictor. **Phase 4 (Hard sync)**. An instantaneous parameter copy from online to target eliminates any residual mismatch before native rollout resumes. **Phase 5 (Finalize)**. The predictor is trained on the now-stabilized encoder under native autoregressive rollout — the same regime as inference — using the remaining compute budget to fully converge the predictor on the refined encoder representations. Each phase prevents a specific failure mode that emerges if it is removed; §5.2 reports a five-paradigm ablation empirically validating each component.

Together, the co-training objective (§4.1) and five-phase curriculum (§4.2) constitute CLIN-JEPA’s complete pretraining recipe; §5 characterizes the resulting model’s behavior across three independent evaluation axes.

5 Experiments

We evaluate CLIN-JEPA on MIMIC-IV ICU [10] along three independent axes, in the order *train* → *diagnose* → *apply*: §5.2 *proves* the co-training paradigm is stable and converges, §5.3 *diagnoses* the latent geometry the encoder learns, and §5.4 *applies* the learned representation to downstream multi-task evaluation. All three axes independently support CLIN-JEPA over prior JEPA-family designs, ablations of our own curriculum, and strong tabular and sequence baselines.

5.1 Setup

Datasets. All experiments use MIMIC-IV ICU [10], with 84,497 stays from 64,874 unique patients. We split at the *patient* level (70/15/15 train/val/test): all ICU stays from a given patient are assigned to the same split, preventing patient-level data leakage between train, validation, and test. Per-hour state and action representations are constructed from MIMIC-IV’s raw tables and the official `mimic-code` derived concept tables; the complete list of source tables and observation/action features is provided in Appendix A. Each stay is windowed at 1-hour resolution following §3.1 ($T_{\max}=72$); stays exceeding 72 hours yield overlapping windows at stride 12 hours, totaling $\sim 197\text{K}$ training windows.

Pretraining. CLIN-JEPA pretraining follows the five-phase curriculum of §4 (predictor warmup, co-training, alignment, hard sync, finalize), executed on $8\times$ NVIDIA H200 GPUs for ~ 54 GPU-hours. Full optimizer and architecture hyperparameters are deferred to Appendix B.

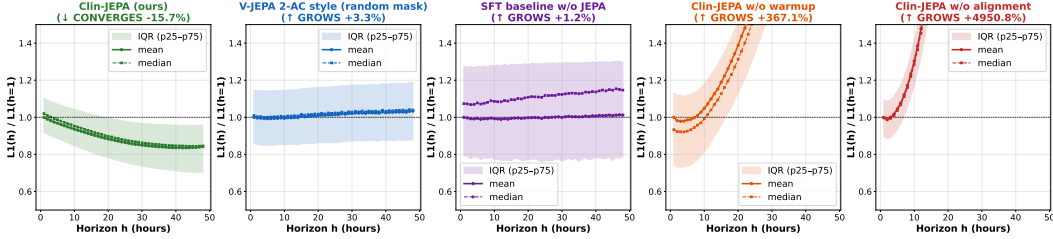
Downstream baselines. For downstream evaluation (§5.4), we compare against four standard strong baselines from the clinical-ML literature: Ridge regression, LightGBM [29], LSTM [30], and TCN [31], trained on raw clinical features.

Curriculum ablation variants. For curriculum ablation (§5.2), we compare CLIN-JEPA against four training-paradigm variants: V-JEPA 2-AC style [9] (random-mask JEPA followed by AC-predictor training on the frozen encoder), SFT baseline w/o JEPA refinement (encoder uses only the §3.1 SFT-initialized LoRA), CLIN-JEPA w/o warmup (Phase 1 removed), and CLIN-JEPA w/o alignment (Phases 3 and 4 removed). All five paradigms share the SFT-initialized encoder and the same 92M predictor architecture; they differ only in the encoder training objective.

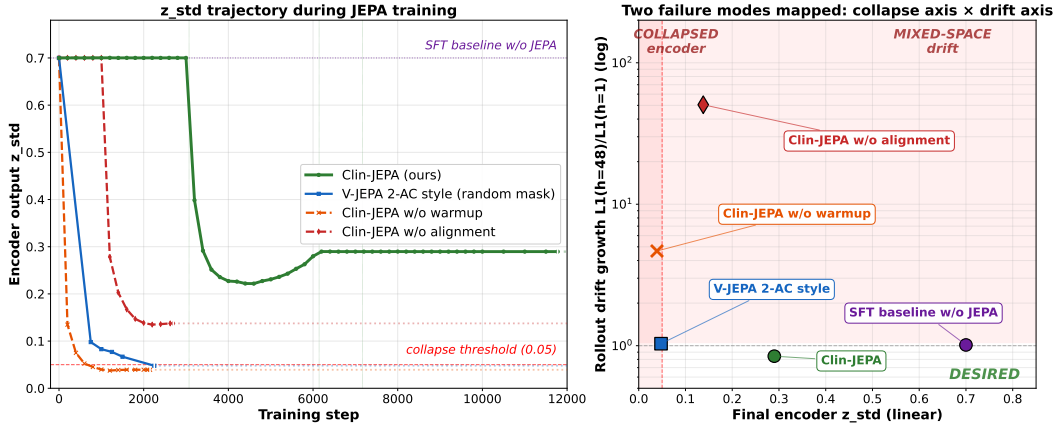
5.2 Co-Training Stability and Convergence

We measure training stability through two signals: *rollout drift* — the L1 distance between the predictor’s autoregressive output \hat{z}_{C+h} and the encoder’s true forward output z_{C+h} over a 48-hour horizon, normalized by the $h=1$ value; and *representation collapse* — the standard deviation of encoder output (z_{std} , a standard self-supervised representation-collapse indicator [7, 8]), tracking whether the encoder degenerates to constant outputs. Across the five training paradigms defined in §5.1, only CLIN-JEPA produces a converging, non-collapsing latent trajectory.

CLIN-JEPA uniquely converges over long horizons. Over the 48-hour rollout horizon, CLIN-JEPA’s mean rollout error *decreases* by -15.7% relative to its $h=1$ value (Figure 2a), while V-JEPA 2-AC style is essentially flat ($+3.4\%$) and the SFT baseline shows modest divergence ($+6.8\%$ median). Both ablations diverge catastrophically: removing warmup yields $+367\%$ drift accumulation, and removing alignment yields $+4951\%$. The convergence pattern in CLIN-JEPA reflects an underlying clinical reality: most ICU patients in our test set transition toward a relatively stable physiological



(a) Error accumulation in predictor-simulated latent trajectories.



(b) Representation collapse and rollout drift as independent failure modes.

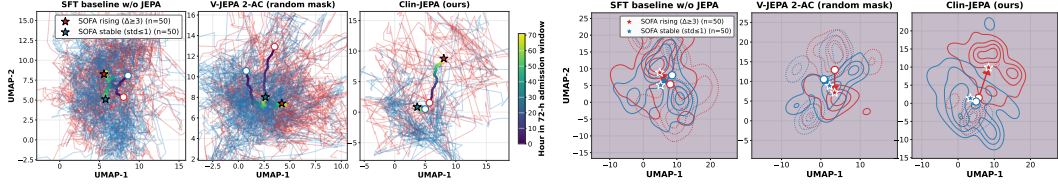
Figure 2: **Co-training stability and convergence across five training paradigms.** (a) Per-paradigm rollout error accumulation: mean drift trajectory with IQR shading (chosen over standard deviation for robustness to heavy-tailed drift in failure-mode paradigms) for each of the five training paradigms, evaluated at context $C=24$ on the held-out test split. Drift is the L1 distance between the predictor’s autoregressive output and the encoder’s true forward output, normalized by the $h=1$ value. (b) *Left*: z_{std} trajectory during JEPA refinement, exposing representation collapse for paradigms that lack the warmup phase. (b) *Right*: joint distribution of final z_{std} (x -axis) and drift accumulation (y -axis) across paradigms, showing collapse and drift are independent failure modes; only CLIN-JEPA occupies the desired (high- z_{std} , low-drift) quadrant.

attractor near end-of-stay (recovery to baseline, transition to comfort care, or pre-discharge stable state), while early hours are dominated by acute decompensation and rapid intervention response. A predictor that has learned the underlying clinical dynamics should therefore predict late-horizon states more accurately than early-horizon ones — exactly the pattern CLIN-JEPA exhibits. Baselines and ablations that fail to learn the dynamics either drift or remain flat across horizon.

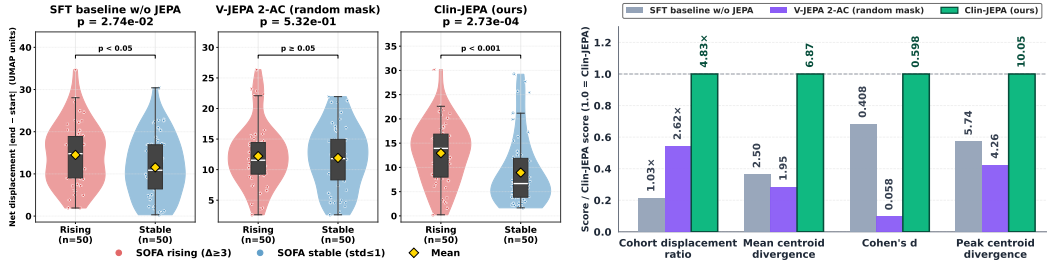
Every component of the curriculum is necessary. *Without warmup* (V-JEPA 2-AC style and CLIN-JEPA w/o warmup), the encoder collapses during early JEPA refinement: z_{std} drops below 0.05 — about 7% of the SFT-pretrained baseline ($z_{\text{std}}=0.700$) and the operational threshold below which downstream linear probes fail to converge (Figure 2b, left). The two warmup-protected variants (CLIN-JEPA and CLIN-JEPA w/o alignment) maintain healthy z_{std} throughout training. *Without alignment* (CLIN-JEPA w/o alignment), the predictor instead learns to map online-space contexts to target-space outputs, then chains those outputs back as online-space inputs at the next rollout step, compounding error across the rollout horizon. Together, the drift evidence in Figure 2a and the collapse evidence in Figure 2b (left) expose two independent failure modes (Figure 2b, right): only CLIN-JEPA, with both warmup and alignment, occupies the desired (high- z_{std} , low-drift) quadrant.

5.3 Latent Geometry Diagnosis

§5.2 established that CLIN-JEPA trains stably; we now ask what its encoder *learned*. Following the JEPA family’s standard evaluation axis [7–9], we probe encoder representation geometry directly — the upstream bottleneck for our retained-predictor design (§3.2). From the test set, we identify two extreme phenotypes — 50 *deteriorating* patients (progressive organ failure: $\Delta\text{SOFA} \geq 3$ over



(a) **Trajectories.** Per-encoder trajectories with cohort means highlighted along a time-coded color band (hour 0→71). (b) **Density contours.** Admission (dotted) vs. end-of-window (filled) cohort distributions; arrows mark mean displacement.



(c) **Per-patient net-displacement distributions.** One-sided Mann-Whitney U-test brackets and Cohen's d . (d) **Four cross-encoder summary metrics:** cohort displacement ratio, mean centroid divergence, Cohen's d on net displacement, and peak centroid divergence.

Figure 3: **Latent-geometry diagnosis: deteriorating-vs-stable cohort discrimination across three encoder variants.** Each subfigure (a–d) shows one analysis view comparing the same three encoders. Only CLIN-JEPA (ours) produces a clinically discriminative latent geometry.

72 h) and 50 *stable* patients (constant disease severity) — and project each patient's per-hour 4096-dim embeddings through per-encoder UMAP fits (Figure 3). Across all four analysis views, only CLIN-JEPA produces a clinically discriminative latent geometry.

Visual separation is immediately apparent. Figure 3a traces 100 individual patient trajectories per encoder over the 72-hour window: under CLIN-JEPA, the deteriorating and stable cohort means visibly diverge as the window unfolds, while V-JEPA 2-AC style keeps both cohort means tightly clustered together and SFT drifts them apart without recognizable cohort-level structure. Figure 3b makes the same separation distributional: CLIN-JEPA's admission contours (dotted) and end-of-window contours (filled) for the two cohorts barely overlap, with markedly asymmetric cohort-mean displacement arrows; the two baseline encoders show extensive admission/end overlap and near-symmetric arrow lengths. Quantification (panels c–d) confirms what is visible by eye.

The deeper signature: stable patients staying put. The diagnostic of a clinically grounded encoder is not how far deteriorating patients move, but how steady stable patients are kept — a naïve encoder would let every patient's latent representation drift from accumulated noise alone. The cohort displacement ratio — how far the deteriorating cohort centroid moves over 72 hours, divided by how far the stable cohort centroid moves — is $4.83\times$ for CLIN-JEPA, $2.62\times$ for V-JEPA 2-AC style, and $1.03\times$ for SFT (Figure 3d). CLIN-JEPA barely moves stable patients while letting deteriorating patients traverse a long arc; SFT drifts both cohorts almost equally, suggesting its latent dynamics are dominated by representation noise rather than learned clinical structure. Per-patient net-displacement separation reaches Cohen's $d=0.598$ (medium-large effect, $p=2.7 \times 10^{-4}$) for CLIN-JEPA, versus $d=0.058$ (n.s., $p=0.53$) for V-JEPA 2-AC style and $d=0.408$ (small-medium, $p=0.027$) for SFT (Figure 3c). Cohen's d being standardized confirms the $\sim 10\times$ gap over V-JEPA 2-AC is real, not a UMAP scale artefact.

Discriminative power grows with observation horizon. CLIN-JEPA's two cohort centroids reach maximum divergence of 10.05 UMAP units at hour 66 with a mean of 6.87 over the 72-hour window — the encoder distinguishes deterioration from stability *most clearly near the end* of the window. This temporal pattern mirrors the terminal-state convergence observed in §5.2: both reflect that CLIN-JEPA's encoder has internalized the slow, integrative timescale of ICU progression. V-JEPA 2-AC style instead peaks early (hour 27, divergence 4.26) and converges back; SFT drifts apart slowly without clear progression (mean 2.50). V-JEPA 2-AC's early-peak-then-collapse pattern

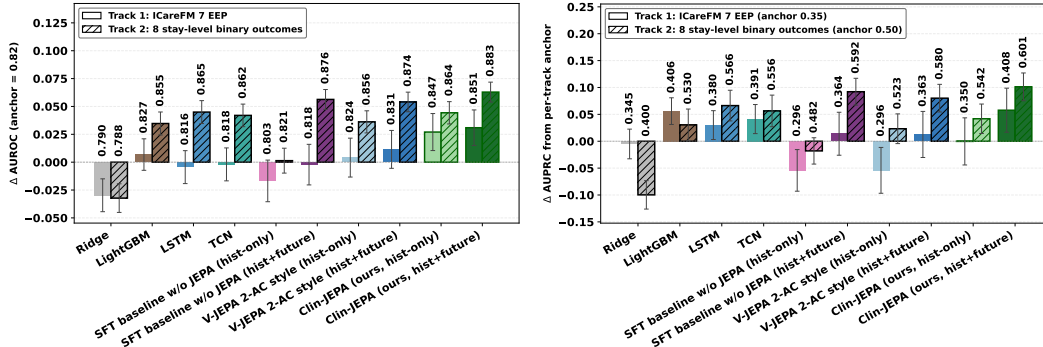


Figure 4: **Downstream multi-task evaluation across two clinical benchmarks.** Mean AUROC (left) and AUPRC (right) per method; paired bars are *Track 1 ICareFM EEP* (solid) and *Track 2 stay-level binary risk* (hatched). CLIN-JEPA (**ours**) with z_{full} leads AUROC on both tracks and AUPRC on Track 2; Track 1 AUPRC ties the strongest baseline.

has a structural cause: its bidirectional masked-reconstruction pretraining never sees the rollout signal, removing the incentive to preserve cohort separation under long-horizon AR composition. CLIN-JEPA’s curriculum is the only paradigm we tested whose discriminative power *grows* with horizon—the property an inference-time autoregressive simulator requires, quantified downstream in §5.4.

5.4 Downstream Multi-Task Evaluation

Setup. We *apply* the deployed CLIN-JEPA model (encoder + retained predictor) to two complementary clinical task families. *Track 1* — *ICareFM Early Event Prediction (EEP)* [5] comprises 7 multi-criteria event-prediction tasks (circulatory, respiratory, kidney, liver, hyperglycemia, sepsis-3, decompensation) at horizons of 8–48 hours. *Track 2* — *a stay-level clinical risk benchmark* [1–4] comprises 8 admission-anchored binary outcomes (six mortality variants, prolonged-stay-7d, and sepsis-ever) on 10,346 test stays. Both tracks fix the encoder context length to $C=24$ hours. Whereas the four baselines (§5.1) are retrained per-task on hand-engineered features, CLIN-JEPA’s deployed model serves all 15 tasks from a single set of latent embeddings without per-task fine-tuning.

Probe. For each task, a shallow MLP probe (one hidden layer with ReLU) is trained on two feature configurations: a *history-only* variant z_{hist} that pools the encoder’s embeddings of the 24-hour context (state, action, and statics), and a *history-plus-future* variant $z_{\text{full}} = z_{\text{hist}} \oplus z_{\text{fut}}$, where z_{fut} pools the encoder’s embeddings of the predictor’s autoregressive rollout over the remaining trajectory. The same probe architecture is used across all encoder variants and both task tracks for fair comparison.

CLIN-JEPA leads both tracks. On Track 1 (Figure 4), CLIN-JEPA’s z_{full} reaches mean AUROC **0.851**, exceeding the strongest baseline LightGBM (0.827) by +0.024 and both encoder ablations (V-JEPA 2-AC 0.831, SFT 0.818). On Track 2 it reaches **0.883**, beating LSTM (0.865) by +0.018. Track 2 AUPRC follows the same ordering (**0.601** vs. 0.566, +0.035); Track 1 AUPRC ties at the mean (0.408 vs. 0.406)—the AUROC–AUPRC divergence reflects LightGBM’s strength on low-base-rate threshold tasks. Per-task tables and 95% bootstrap CIs in Appendix C.

The retained predictor adds value. The $z_{\text{hist}} \rightarrow z_{\text{full}}$ transition isolates the predictor’s contribution: on Track 2, lift is +0.019 mean AUROC with CLIN-JEPA winning **all 8 of 8 outcomes**—confirming retained-predictor value beyond the §5.2 latent-rollout metric.

Where the representation pays off. CLIN-JEPA’s gains concentrate on tasks that require composing heterogeneous trajectory information into a coherent clinical assessment: kidney injury (+0.111 AUROC vs. LightGBM), sepsis-3 (+0.057), and decompensation (+0.189) on Track 1, and prolonged-stay-7d (+0.087 vs. LSTM) and sepsis-ever (+0.068) on Track 2. On simpler threshold-detection or acuity-driven tasks, feature-engineered baselines already extract close-to-sufficient signal from raw vital trends, and CLIN-JEPA matches them within bootstrap CI rather than dominating. The pattern is systematic: gains where temporal composition matters, ties where it does not.

6 Conclusion

We presented CLIN-JEPA, a multi-phase co-training framework for joint-embedding predictive pretraining on EHR patient trajectories. Our curriculum closes the gap left by prior JEPA designs that either discard the predictor or train it on a frozen encoder. To our knowledge, this is the first framework where a single clinical backbone delivers stable autoregressive rollout, clinically discriminative latent geometry, and competitive multi-task downstream performance from one set of latent embeddings.

Acknowledgments and Disclosure of Funding

This work was supported by the National Institutes of Health under Award Numbers GM139967 and HL170175. Computational resources were provided by the Duke Compute Cluster (DCC) and the NCSHare research-computing infrastructure. We thank the MIMIC-IV team at the MIT Laboratory for Computational Physiology and Beth Israel Deaconess Medical Center for making the dataset publicly available.

References

- [1] Nikita Makarov, Maria Bordukova, Papichaya Quengdaeng, Daniel Garger, Raul Rodriguez-Esteban, Fabian Schmich, and Michael P Menden. Large language models forecast patient health trajectories enabling digital twins. *npj Digital Medicine*, 8(1):588, 2025.
- [2] Pawel Renc, Yugang Jia, Anthony E Samir, Jaroslaw Was, Quanzheng Li, David W Bates, and Arkadiusz Sitek. Zero shot health trajectory prediction using transformer. *NPJ digital medicine*, 7(1):256, 2024.
- [3] Zhenbang Wu, Anant Dadu, Mike Nalls, Faraz Faghri, and Jimeng Sun. Instruction tuning large language models to understand electronic health records. *Advances in Neural Information Processing Systems*, 37: 54772–54786, 2024.
- [4] Yusheng Liao, Chaoyi Wu, Junwei Liu, Shuyang Jiang, Pengcheng Qiu, Haowen Wang, Yun Yue, Shuai Zhen, Jian Wang, Qianrui Fan, et al. Ehr-r1: A reasoning-enhanced foundational language model for electronic health record analysis. *arXiv preprint arXiv:2510.25628*, 2025.
- [5] Manuel Burger, Daphné Chopard, Gregor Lichtner, Malte Londschieen, Fedor Sergeev, Moritz Fuchs, Hugo Yèche, Rita Kuznetsova, Martin Faltys, Eike Gerdes, et al. A foundation model for intensive care: Unlocking generalization across tasks and domains at scale. *medRxiv*, pages 2025–07, 2025.
- [6] Yann LeCun et al. A path towards autonomous machine intelligence version 0.9. 2, 2022-06-27. *Open Review*, 62(1):1–62, 2022.
- [7] Mahmoud Assran, Quentin Duval, Ishan Misra, Piotr Bojanowski, Pascal Vincent, Michael Rabbat, Yann LeCun, and Nicolas Ballas. Self-supervised learning from images with a joint-embedding predictive architecture. In *Proceedings of the IEEE/CVF conference on computer vision and pattern recognition*, pages 15619–15629, 2023.
- [8] Adrien Bardes, Quentin Garrido, Jean Ponce, Xinlei Chen, Michael Rabbat, Yann LeCun, Mahmoud Assran, and Nicolas Ballas. Revisiting feature prediction for learning visual representations from video. *arXiv preprint arXiv:2404.08471*, 2024.
- [9] Mido Assran, Adrien Bardes, David Fan, Quentin Garrido, Russell Howes, Matthew Muckley, Ammar Rizvi, Claire Roberts, Koustuv Sinha, Artem Zhohus, et al. V-jepa 2: Self-supervised video models enable understanding, prediction and planning. *arXiv preprint arXiv:2506.09985*, 2025.
- [10] Alistair EW Johnson, Lucas Bulgarelli, Lu Shen, Alvin Gayles, Ayad Shammout, Steven Horng, Tom J Pollard, Sicheng Hao, Benjamin Moody, Brian Gow, et al. Mimic-iv, a freely accessible electronic health record dataset. *Scientific data*, 10(1):1, 2023.
- [11] Laila Rasmy, Yang Xiang, Ziqian Xie, Cui Tao, and Degui Zhi. Med-bert: pretrained contextualized embeddings on large-scale structured electronic health records for disease prediction. *NPJ digital medicine*, 4(1):86, 2021.
- [12] Xi Yang, Aokun Chen, Nima PourNejatian, Hoo Chang Shin, Kaleb E Smith, Christopher Parisien, Colin Compas, Cheryl Martin, Anthony B Costa, Mona G Flores, et al. A large language model for electronic health records. *NPJ digital medicine*, 5(1):194, 2022.
- [13] Zeljko Kraljevic, Dan Bean, Anthony Shek, Rebecca Bendayan, Harry Hemingway, Joshua Au Yeung, Alexander Deng, Alfred Balston, Jack Ross, Esther Idowu, et al. Foresight—a generative pretrained transformer for modelling of patient timelines using electronic health records: a retrospective modelling study. *The Lancet Digital Health*, 6(4):e281–e290, 2024.
- [14] Adibvafa Fallahpour, Mahshid Alinoori, Wenqian Ye, Xu Cao, Arash Afkanpour, and Amrit Krishnan. Ehrmamba: Towards generalizable and scalable foundation models for electronic health records. *arXiv preprint arXiv:2405.14567*, 2024.
- [15] Hejie Cui, Alyssa Unell, Bowen Chen, Jason Alan Fries, Emily Alsentzer, Sanmi Koyejo, and Nigam H Shah. Timer: Temporal instruction modeling and evaluation for longitudinal clinical records. *npj Digital Medicine*, 8(1):577, 2025.
- [16] Zekai Chen, Arda Pekis, and Kevin Brown. Building the ehr foundation model via next event prediction. *arXiv preprint arXiv:2509.25591*, 2025.
- [17] Pawel Renc, Michal K Grzeszczyk, Nassim Oufattole, Deirdre Goode, Yugang Jia, Szymon Bieganski, Matthew BA McDermott, Jaroslaw Was, Anthony E Samir, Jonathan W Cunningham, et al. Foundation model of electronic medical records for adaptive risk estimation. *GigaScience*, 14:giaf107, 2025.

- [18] Michael C Burkhart, Bashar Ramadan, Zewei Liao, Kaveri Chhikara, Juan C Rojas, William F Parker, and Brett K Beaulieu-Jones. Foundation models for electronic health records: representation dynamics and transferability. *arXiv preprint arXiv:2504.10422*, 2025.
- [19] Hai Huang, Yann LeCun, and Randall Balestriero. Llm-jepa: Large language models meet joint embedding predictive architectures. *arXiv preprint arXiv:2509.14252*, 2025.
- [20] DeLong Chen, Mustafa Shukor, Theo Moutakanni, Willy Chung, Jade Yu, Tejaswi Kasarla, Yejin Bang, Allen Bolourchi, Yann LeCun, and Pascale Fung. Vl-jepa: Joint embedding predictive architecture for vision-language. *arXiv preprint arXiv:2512.10942*, 2025.
- [21] Irsyad Adam, Zekai Chen, David Laprade, Shaun Porwal, David Laub, Erik Reinertsen, Arda Pekis, and Kevin Brown. The patient is not a moving document: A world model training paradigm for longitudinal ehr. *arXiv preprint arXiv:2601.22128*, 2026.
- [22] Qianyi Xu, Gousia Habib, Feng Wu, Dilruk Perera, and Mengling Feng. Meddreamer: Model-based reinforcement learning with latent imagination on complex ehRs for clinical decision support. In *Proceedings of the 32nd ACM SIGKDD Conference on Knowledge Discovery and Data Mining V. 1*, pages 1693–1704, 2026.
- [23] Danijar Hafner, Timothy Lillicrap, Mohammad Norouzi, and Jimmy Ba. Mastering atari with discrete world models. *arXiv preprint arXiv:2010.02193*, 2020.
- [24] Shane Lowe, Garrett Park, Liam Lee, and Parker Smith. Latent physiology as language: A state-space foundation model for multimodal icu and ehr representation learning.
- [25] Tianxingjian Ding, Yuanhao Zou, Chen Chen, Mubarak Shah, and Yu Tian. Clarity: Medical world model for guiding treatment decisions by modeling context-aware disease trajectories in latent space. *arXiv preprint arXiv:2512.08029*, 2025.
- [26] Mohammad Areeb Qazi, Maryam Nadeem, and Mohammad Yaqub. Beyond generative ai: World models for clinical prediction, counterfactuals, and planning. *arXiv preprint arXiv:2511.16333*, 2025.
- [27] Hrayr Harutyunyan, Hrant Khachatryan, David C Kale, Greg Ver Steeg, and Aram Galstyan. Multitask learning and benchmarking with clinical time series data. *Scientific data*, 6(1):96, 2019.
- [28] Sanjay Purushotham, Chuizheng Meng, Zhengping Che, and Yan Liu. Benchmarking deep learning models on large healthcare datasets. *Journal of biomedical informatics*, 83:112–134, 2018.
- [29] Guolin Ke, Qi Meng, Thomas Finley, Taifeng Wang, Wei Chen, Weidong Ma, Qiwei Ye, and Tie-Yan Liu. Lightgbm: A highly efficient gradient boosting decision tree. *Advances in neural information processing systems*, 30, 2017.
- [30] Sepp Hochreiter and Jürgen Schmidhuber. Long short-term memory. *Neural computation*, 9(8):1735–1780, 1997.
- [31] Shaojie Bai, J Zico Kolter, and Vladlen Koltun. An empirical evaluation of generic convolutional and recurrent networks for sequence modeling. *arXiv preprint arXiv:1803.01271*, 2018.

Appendix

A Source tables and feature inventory

This appendix documents the MIMIC-IV [10] source tables and the per-hour features used to construct the encoder’s state and action text inputs (§3.1). Source tables prefixed `concepts.*` are official `mimic-code` derived concept tables; remaining sources (`inputevents`, `prescriptions`, `procedureevents`, ...) are MIMIC-IV raw tables.

Inclusion criteria. ICU stays included in the cohort satisfy: age ≥ 18 , ICU length of stay ≥ 6 hours, and ≥ 1 observation event. Trajectory windows are capped at $T_{\max}=72$ hours (1-hour discretization); stays exceeding 72 hours yield overlapping windows at stride 12 hours.

Table 2: Observation features (patient state) extracted from MIMIC-IV. Source tables prefixed `concepts.*` are official `mimic-code` derived concepts; raw tables are from MIMIC-IV directly.

Domain	Source table	Category	Variables
vitalsign	<code>concepts.measurement.vitalsign</code>	vitals	heart_rate, sbp, dbp, mbp, sbp_ni, dbp_ni, mbp_ni, resp_rate, temperature, spo2, glucose
bg	<code>concepts.measurement.bg</code>	blood_gas	so2, po2, pco2, fio2, fio2_chartevents, ph, baseexcess, bicarbonate, totalco2, hematocrit, hemoglobin, chloride, calcium, potassium, sodium, lactate, glucose, aado2, aado2_calc, pao2fio2ratio
chemistry	<code>concepts.measurement.chemistry</code>	labs	albumin, globulin, total_protein, aniongap, bicarbonate, bun, calcium, chloride, creatinine, glucose, sodium, potassium
complete_blood_count	<code>concepts.measurement.complete_blood_count</code>	labs	hematocrit, hemoglobin, mch, mhc, mcv, platelet, rbc, rdw, rdwsd, wbc
coagulation	<code>concepts.measurement.coagulation</code>	labs	d_dimer, fibrinogen, thrombin, inr, pt, ptt
enzyme	<code>concepts.measurement.enzyme</code>	labs	a, l, l
inflammation	<code>concepts.measurement.inflammation</code>	labs	a, l, l
cardiac_marker	<code>concepts.measurement.cardiac_marker</code>	labs	a, l, l
gcs	<code>concepts.measurement.gcs</code>	assessment	a, l, l
urine_output	<code>concepts.measurement.urine_output</code>	output	urineoutput
urine_output_rate	<code>concepts.measurement.urine_output_rate</code>	output	uo, urineoutput_6hr, urineoutput_12hr, urineoutput_24hr, uo_mlg_6hr, uo_mlg_12hr, uo_mlg_24hr, weight

Continued on next page...

(Table 2 continued)

Domain	Source table	Category	Variables
kdigo_stages	concepts.organfailure.kdigo_stages	organ_failure	creat, creat_low_past_7day, creat_low_past_48hr, aki_stage_creat, uo_rt_6hr, uo_rt_12hr, uo_rt_24hr, aki_stage_uo, aki_stage_crrt, aki_stage, aki_stage_smoothed
oxygen_delivery	concepts.measurement.oxygen_delivery	vitals	o2_flow, o2_flow_additional, o2_delivery_device_1
blood_differential	concepts.measurement.blood_differential	labs	wbc, neutrophils_abs, lymphocytes_abs, monocytes_abs, eosinophils_abs, basophils_abs, bands, immature_granulocytes, nrbc
height	concepts.measurement.height	vitals	height
weight	concepts.demographics.weight_durations	vitals	weight, weight_type
sofa	concepts.score.sofa	score	sofa_24hours, res- piration_24hours, coagulation_24hours, liver_24hours, car- diovascular_24hours, cns_24hours, re- nal_24hours
rhythm	concepts.measurement.rhythm	vitals	heart_rhythm, ectopy_type, ec- topy_frequency

Table 3: Action features (clinical interventions) extracted from MIMIC-IV. Source tables prefixed concepts.* are official mimic-code derived concepts; inpatientevents, prescriptions, etc. are MIMIC-IV raw tables.

Domain	Source table	Category	Variables
vasoactive_agent	concepts.medication.vasoactive_agent	vasopressor	dopamine, epinephrine, nore- pinephrine, phenyle- phrine, vaso- pressin, dobu- tamine, milri- none
norepinephrine_equivalent_dose	concepts.medication.norepinephrine_equivalent_dose	vasopressor	norepinephrine_equivalent_dose
antibiotic	concepts.medication.antibiotic	antibiotic	antibiotic, route
ventilation	concepts.treatment.ventilation	ventilation	ventilation_status
ventilator_setting	concepts.measurement.ventilator_setting	ventilation_settings	a, l, l
rrt	concepts.treatment.rrt	dialysis	dialysis_present, dialy- sis_active, dialy- sis_type
crrt	concepts.treatment.crrt	dialysis	a, l, l
invasive_line	concepts.treatment.invasive_line	procedure	a, l, l

Continued on next page...

(Table 3 continued)

Domain	Source table	Category	Variables
neuroblock	concepts.medication.neuroblock	neuromuscular_blocker	drug_rate, drug_amount

B Training hyperparameters

Table 4 lists all hyperparameters used in CLIN-JEPA pretraining (§4). The encoder LoRA is first SFT-initialized via per-hour next-token prediction on state and action text (§3.1), then refined jointly with the predictor under the five-phase curriculum (§4.2).

Table 4: Full hyperparameters for CLIN-JEPA training pipeline.

Stage / component	Parameter	Value
Encoder (architecture)	Base model	Qwen3-8B (8.2B parameters, 4096-dim hidden)
	LoRA rank r	16
	LoRA α	32
	LoRA target modules	<code>q_proj, k_proj, v_proj, o_proj</code>
	Trainable parameters	$\sim 30.7\text{M}$ (0.37% of base)
	Embedding extraction	last-token hidden state (4096-dim)
	Max sequence length	4096 tokens
	Attention impl.	Flash Attention 2
Predictor (architecture)	Architecture	Transformer encoder, pre-norm GELU
	Layers	6
	Hidden dimension	1024
	Attention heads	8
	FFN dimension	4096
	FFN dropout	0.15
	Attention dropout	0.10
	Positional encoding	learned absolute, max sequence length 149
	Output mode	absolute (not residual)
Total parameters	92.5M	
SFT initialization	Optimizer	AdamW
	Learning rate	$1e-4$
	LR schedule	cosine
	Epochs	1
	Sample format	per-(stay, hour) state OR action text (independent samples)
JEPA pretraining (curriculum)	Optimizer	AdamW
	Encoder learning rate	$5e-5$
	Predictor learning rate	$5e-4$
	LR schedule	cosine, 2% warmup over total steps
	Weight decay	0.04
	Gradient clip (encoder)	0.5
	Gradient clip (predictor)	1.0
	Effective batch	64 trajectory windows per step (8 GPUs \times 8 per-GPU)
	Total optimizer steps	$\sim 11,776$ (≈ 3.83 epochs over 197K-window train set)
	Phase schedule	Phase 1 (warmup): 3072 steps; Phase 2 (co-training): 3072; Phase 3 (alignment): 1024; Phase 4 (hard sync): instantaneous; Phase 5 (finalize): 4608
	Rollout horizon	2 steps
	Loss	ℓ_1 teacher-forcing + 2-step rollout (Eq. 5)
	EMA momentum τ	0.996 (fixed in Phases 2 and 3)
	EMA precision	fp32 (online encoder bf16)
	Random seed	42
	Hardware	8 \times NVIDIA H200
	Wall-clock	~ 54 GPU-hours

C Per-task downstream results

Full per-task tables for the downstream evaluation in §5.4. Bootstrap 95% confidence intervals computed from $n_{\text{boot}}=500$ resamples clustered by stay. Bolded cells indicate the per-column maximum.

Table 5: **Track 1: ICareFM 7 EEP tasks — AUROC (95% CI), $C=24\text{h}$.** Higher is better. Best per task in bold.

Method	Circulatory 8h	Respiratory 24h	Kidney 48h	Liver 48h	Hyperglycemia 8h	Sepsis-3 8h	Decomp 24h	Mean
Ridge	0.955 [0.948,0.961]	0.783 [0.764,0.800]	0.696 [0.679,0.712]	0.948 [0.938,0.956]	0.647 [0.633,0.660]	0.693 [0.669,0.721]	0.809 [0.795,0.823]	0.790
LightGBM	0.975 [0.969,0.979]	0.794 [0.776,0.812]	0.686 [0.670,0.702]	0.960 [0.951,0.967]	0.846 [0.838,0.853]	0.723 [0.690,0.754]	0.804 [0.791,0.816]	0.827
LSTM	0.965 [0.959,0.970]	0.791 [0.773,0.809]	0.718 [0.702,0.736]	0.953 [0.943,0.961]	0.681 [0.668,0.695]	0.738 [0.709,0.766]	0.862 [0.848,0.873]	0.816
TCN	0.964 [0.957,0.969]	0.790 [0.770,0.808]	0.723 [0.705,0.738]	0.952 [0.943,0.960]	0.676 [0.663,0.689]	0.752 [0.724,0.782]	0.869 [0.856,0.880]	0.818
SFT w/o JEPA (hist-only)	0.881 [0.863,0.897]	0.593 [0.565,0.621]	0.790 [0.776,0.805]	0.889 [0.869,0.904]	0.749 [0.735,0.761]	0.744 [0.712,0.777]	0.976 [0.968,0.983]	0.803
SFT w/o JEPA (hist+fut)	0.882 [0.864,0.898]	0.729 [0.707,0.752]	0.802 [0.788,0.816]	0.886 [0.867,0.902]	0.743 [0.729,0.756]	0.691 [0.653,0.727]	0.991 [0.984,0.996]	0.818
V-JEPA 2-AC (hist-only)	0.877 [0.858,0.892]	0.755 [0.731,0.777]	0.793 [0.777,0.807]	0.897 [0.879,0.911]	0.726 [0.712,0.740]	0.747 [0.717,0.780]	0.974 [0.969,0.980]	0.824
V-JEPA 2-AC (hist+fut)	0.876 [0.858,0.892]	0.759 [0.737,0.782]	0.810 [0.797,0.824]	0.900 [0.884,0.914]	0.724 [0.709,0.738]	0.757 [0.724,0.791]	0.993 [0.990,0.996]	0.831
Clin-JEPA (hist-only)	0.894 [0.878,0.910]	0.773 [0.750,0.793]	0.787 [0.773,0.803]	0.911 [0.896,0.924]	0.811 [0.798,0.822]	0.776 [0.744,0.808]	0.976 [0.970,0.982]	0.847
Clin-JEPA (hist+fut)	0.894 [0.878,0.908]	0.773 [0.750,0.792]	0.797 [0.783,0.813]	0.911 [0.895,0.924]	0.809 [0.797,0.821]	0.780 [0.748,0.810]	0.993 [0.989,0.996]	0.851

Table 6: **Track 1 (cont.): ICareFM 7 EEP tasks — AUPRC (95% CI), $C=24\text{h}$.** Higher is better. Best per task in bold.

Method	Circulatory 8h	Respiratory 24h	Kidney 48h	Liver 48h	Hyperglycemia 8h	Sepsis-3 8h	Decomp 24h	Mean
Ridge	0.719 [0.679,0.752]	0.278 [0.244,0.315]	0.222 [0.198,0.244]	0.709 [0.652,0.751]	0.251 [0.234,0.272]	0.022 [0.018,0.027]	0.214 [0.191,0.240]	0.345
LightGBM	0.788 [0.754,0.817]	0.311 [0.273,0.352]	0.187 [0.166,0.208]	0.803 [0.763,0.835]	0.570 [0.548,0.591]	0.026 [0.020,0.033]	0.159 [0.142,0.178]	0.406
LSTM	0.758 [0.723,0.788]	0.286 [0.251,0.322]	0.221 [0.196,0.243]	0.774 [0.728,0.809]	0.284 [0.262,0.308]	0.027 [0.022,0.035]	0.310 [0.285,0.337]	0.380
TCN	0.759 [0.722,0.787]	0.299 [0.263,0.338]	0.241 [0.216,0.264]	0.778 [0.730,0.813]	0.281 [0.259,0.304]	0.028 [0.022,0.035]	0.354 [0.329,0.380]	0.391
SFT w/o JEPA (hist-only)	0.342 [0.291,0.391]	0.121 [0.101,0.151]	0.285 [0.262,0.310]	0.543 [0.481,0.600]	0.387 [0.358,0.412]	0.043 [0.036,0.057]	0.349 [0.280,0.429]	0.296
SFT w/o JEPA (hist+fut)	0.338 [0.284,0.390]	0.217 [0.181,0.255]	0.301 [0.277,0.326]	0.526 [0.460,0.588]	0.376 [0.347,0.401]	0.038 [0.029,0.056]	0.752 [0.689,0.809]	0.364
V-JEPA 2-AC (hist-only)	0.325 [0.274,0.378]	0.236 [0.195,0.277]	0.295 [0.273,0.323]	0.547 [0.476,0.615]	0.352 [0.325,0.377]	0.050 [0.039,0.074]	0.267 [0.206,0.341]	0.296
V-JEPA 2-AC (hist+fut)	0.316 [0.265,0.368]	0.243 [0.202,0.280]	0.324 [0.299,0.352]	0.549 [0.476,0.621]	0.350 [0.324,0.376]	0.052 [0.040,0.076]	0.705 [0.635,0.766]	0.363
Clin-JEPA (hist-only)	0.370 [0.314,0.430]	0.254 [0.215,0.293]	0.277 [0.255,0.303]	0.644 [0.586,0.702]	0.491 [0.461,0.518]	0.060 [0.044,0.088]	0.352 [0.281,0.436]	0.350
Clin-JEPA (hist+fut)	0.368 [0.317,0.427]	0.258 [0.217,0.296]	0.285 [0.263,0.314]	0.635 [0.573,0.694]	0.489 [0.460,0.515]	0.059 [0.044,0.086]	0.759 [0.700,0.815]	0.408

Table 7: **Track 2: 8 stay-level binary outcomes — AUROC (95% CI), $C=24\text{h}$, admission cohort.** Higher is better. Best per task in bold.

Method	Hosp. mort.	True ICU mort.	Mort 7d	Mort 14d	Mort 30d	Mort 90d	Prolong. stay	Sepsis ever	Mean
Ridge	0.802 [0.789,0.816]	0.828 [0.815,0.841]	0.800 [0.784,0.817]	0.795 [0.782,0.810]	0.783 [0.771,0.797]	0.779 [0.768,0.789]	0.741 [0.727,0.754]	0.774 [0.767,0.782]	0.788
LightGBM	0.866 [0.855,0.876]	0.897 [0.886,0.908]	0.882 [0.870,0.895]	0.860 [0.848,0.871]	0.843 [0.833,0.853]	0.824 [0.815,0.833]	0.822 [0.812,0.834]	0.842 [0.835,0.849]	0.855
LSTM	0.883 [0.871,0.892]	0.907 [0.896,0.917]	0.895 [0.881,0.906]	0.877 [0.866,0.887]	0.861 [0.850,0.871]	0.844 [0.834,0.852]	0.833 [0.822,0.844]	0.821 [0.814,0.829]	0.865
TCN	0.879 [0.868,0.888]	0.905 [0.894,0.915]	0.894 [0.882,0.906]	0.875 [0.864,0.885]	0.858 [0.848,0.869]	0.840 [0.831,0.849]	0.829 [0.818,0.840]	0.816 [0.808,0.824]	0.862
SFT w/o JEPA (hist-only)	0.850 [0.839,0.860]	0.889 [0.878,0.898]	0.602 [0.582,0.623]	0.861 [0.851,0.871]	0.845 [0.834,0.855]	0.828 [0.818,0.837]	0.838 [0.827,0.848]	0.858 [0.850,0.865]	0.821
SFT w/o JEPA (hist+fut)	0.869 [0.858,0.878]	0.906 [0.896,0.914]	0.888 [0.875,0.900]	0.867 [0.857,0.877]	0.854 [0.844,0.864]	0.835 [0.826,0.843]	0.915 [0.910,0.921]	0.877 [0.869,0.883]	0.876
V-JEPA 2-AC (hist-only)	0.859 [0.848,0.869]	0.893 [0.883,0.903]	0.872 [0.859,0.883]	0.859 [0.849,0.869]	0.844 [0.833,0.854]	0.827 [0.817,0.836]	0.839 [0.828,0.849]	0.856 [0.848,0.863]	0.856
V-JEPA 2-AC (hist+fut)	0.870 [0.860,0.879]	0.904 [0.894,0.913]	0.885 [0.872,0.895]	0.867 [0.857,0.877]	0.850 [0.841,0.860]	0.831 [0.822,0.840]	0.918 [0.913,0.923]	0.867 [0.860,0.874]	0.874
Clin-JEPA (hist-only)	0.867 [0.856,0.877]	0.896 [0.885,0.906]	0.877 [0.864,0.889]	0.865 [0.855,0.876]	0.849 [0.839,0.859]	0.834 [0.823,0.842]	0.842 [0.830,0.852]	0.884 [0.878,0.890]	0.864
Clin-JEPA (hist+fut)	0.875 [0.865,0.884]	0.909 [0.900,0.917]	0.890 [0.877,0.901]	0.870 [0.859,0.879]	0.854 [0.844,0.864]	0.836 [0.826,0.845]	0.919 [0.913,0.925]	0.910 [0.904,0.915]	0.883

Table 8: **Track 2 (cont.): 8 stay-level binary outcomes — AUPRC (95% CI), $C=24\text{h}$, admission cohort.** Higher is better. Best per task in bold.

Method	Hosp. mort.	True ICU mort.	Mort 7d	Mort 14d	Mort 30d	Mort 90d	Prolong. stay	Sepsis ever	Mean
Ridge	0.359 [0.331,0.392]	0.328 [0.295,0.364]	0.265 [0.236,0.302]	0.327 [0.301,0.359]	0.394 [0.370,0.423]	0.464 [0.443,0.489]	0.310 [0.290,0.334]	0.755 [0.744,0.767]	0.400
LightGBM	0.499 [0.463,0.529]	0.502 [0.463,0.540]	0.434 [0.395,0.474]	0.480 [0.444,0.515]	0.523 [0.494,0.552]	0.557 [0.533,0.582]	0.423 [0.401,0.452]	0.825 [0.814,0.835]	0.530
LSTM	0.549 [0.517,0.582]	0.537 [0.504,0.578]	0.490 [0.452,0.532]	0.523 [0.492,0.556]	0.567 [0.539,0.594]	0.603 [0.579,0.624]	0.456 [0.433,0.486]	0.805 [0.804,0.815]	0.566
TCN	0.538 [0.503,0.569]	0.528 [0.490,0.565]	0.478 [0.438,0.520]	0.512 [0.478,0.544]	0.554 [0.524,0.580]	0.593 [0.568,0.614]	0.451 [0.425,0.479]	0.797 [0.786,0.808]	0.556
SFT w/o JEPA (hist-only)	0.444 [0.416,0.479]	0.450 [0.416,0.487]	0.099 [0.088,0.114]	0.477 [0.446,0.506]	0.528 [0.501,0.554]	0.564 [0.541,0.588]	0.442 [0.418,0.470]	0.853 [0.843,0.863]	0.482
SFT w/o JEPA (hist+fut)	0.526 [0.497,0.554]	0.542 [0.513,0.575]	0.542 [0.506,0.574]	0.527 [0.498,0.553]	0.569 [0.545,0.590]	0.587 [0.565,0.609]	0.573 [0.549,0.601]	0.873 [0.864,0.881]	0.592
V-JEPA 2-AC (hist-only)	0.472 [0.444,0.500]	0.465 [0.429,0.501]	0.402 [0.364,0.439]	0.463 [0.432,0.492]	0.520 [0.494,0.549]	0.561 [0.539,0.585]	0.452 [0.428,0.482]	0.850 [0.840,0.860]	0.523
V-JEPA 2-AC (hist+fut)	0.524 [0.497,0.551]	0.517 [0.485,0.551]	0.519 [0.485,0.550]	0.523 [0.493,0.552]	0.548 [0.523,0.571]	0.573 [0.552,0.595]	0.575 [0.551,0.605]	0.863 [0.853,0.872]	0.580
Clin-JEPA (hist-only)	0.495 [0.464,0.526]	0.485 [0.450,0.519]	0.433 [0.393,0.468]	0.479 [0.446,0.509]	0.534 [0.507,0.560]	0.573 [0.550,0.596]	0.459 [0.434,0.487]	0.878 [0.869,0.886]	0.542
Clin-JEPA (hist+fut)	0.539 [0.511,0.568]	0.542 [0.509,0.574]	0.549 [0.513,0.580]	0.521 [0.489,0.550]	0.559 [0.533,0.583]	0.590 [0.567,0.612]	0.604 [0.578,0.632]	0.906 [0.898,0.912]	0.601